Enhancement of Sedimentation Velocity of Heavy Metals Loaded Hydroxyapatite Using Chitosan Extracted from Shrimp Waste

Article *in* Journal of Polymers and the Environment · September 2012

DOI: 10.1007/s10924-012-0440-7

CITATIONS
35

READS
626

6 authors, including:

Kadouche Slimane

9 PUBLICATIONS **101** CITATIONS

SEE PROFILE

Hakim Lounici

Université de Bouira

202 PUBLICATIONS **3,560** CITATIONS

SEE PROFILE

Nadjib Drouiche

Centre de Recherche en Technologie des Semi-conducteurs pour l'Energétique (C…

158 PUBLICATIONS **2,689** CITATIONS

SEE PROFILE

Madjid Hadioui

Université de Montréal

30 PUBLICATIONS **343** CITATIONS

SEE PROFILE

J Polym Environ (2012) 20:848–857
DOI 10.1007/s10924-012-0440-7

ORIGINAL PAPER

Enhancement of Sedimentation Velocity of Heavy Metals Loaded Hydroxyapatite Using Chitosan Extracted from Shrimp Waste

S. Kadouche · H. Lounici · K. Benaoumeur · N. Drouiche · M. Hadioui · P. Sharrock

Published online: 21 April 2012

Abstract In this study, synthesize hydroxyapatite (HA) suspensions sedimentation was used after usual terms as support for adsorption of heavy metals ions. Thus, the effectiveness of chitosan, produced from shrimp waste, in the flocculation of turbid suspensions resulting from the treatment of water contaminated with heavy metals was studied by adsorption on HA. Different particles sizes of HA were mainly controlled in this work (an average of granule size ranging from 1.6 to 63 μm). The results of Cu^{2+} and Zn^{2+} adsorption on HA showed relatively fast kinetics, with removal extent of 88–95 % by varying the initial total metal concentration. High removal rates were obtained for Cu^{2+}. Chitosan was found to be able to eliminate by flocculation more than 98 % of turbid suspensions generated by metals adsorption on HA after only 30 min of sedimentation. Effects of pH and dose of chitosan on the coagulation–flocculation process were also studied. The optimal dose of chitosan was found between 0.2 and 2 mg/L which corresponds to an optimal pH ranging from 6 to 7.

Keywords Hydroxyapatite · Chitosan · Coagulation · Sedimentation velocity · Heavy metals

S. Kadouche · M. Hadioui
Faculté des Sciences, UMMTO, Campus Bastos, Tizi Ouzou, Algeria

H. Lounici · K. Benaoumeur
Laboratoire BIOGEP, Ecole Nationale Polytechnique d'Alger, 10 Avenue pasteur El Harrach, Algiers, Algeria

N. Drouiche (✉)
Department of Environmental Engineering, Silicon Technology Development Unit, 2, Bd Frantz Fanon BP140, Alger-7, 16027 Merveilles, Algeria
e-mail: nadjibdrouiche@yahoo.fr

P. Sharrock
LERISM, IUT Paul Sabatier, Université de Toulouse, Castres, France

Introduction

Water is one of the natural renewable resources essential for economic and social development. Over the last decade, environmental pollution was a major global concern. When it sources is enumerated, water pollution by heavy metals and metalloids is, with increasing frequency, listed as a major contributor. Large quantities of waste are continuously discharged into the environment by mining processes. Heavy metals are released into the environment by aforementioned anthropogenic activities. It can also occur naturally in the soil environment from the pedogenetic processes of weathering of parent materials at levels.

Various treatment technologies have been developed for the purification of water and wastewater contaminated by heavy metals. The most commonly used methods for the removal of heavy metals ions from water include: chemical precipitation, solvent extraction, adsorption, filtration flocculation, sedimentation, etc. Among these, adsorption has evolved as the front line of defense and especially for those, which cannot be removed by other techniques.

Generally, adsorption treatments using activated carbons are the most widely used for removing heavy metals ions from water. Recently, numerous approaches have been studied for the development of cheaper and more effective adsorbents containing natural products. Among these, calcium Hydroxyapatite (HA) deserves particular attention. Hence adsorption on hydroxyapatite can be a low cost

procedure of choice in water decontamination for extraction and separation of heavy metals ions.

Several authors had already investigated the retention of heavy metal ions on either synthetic [1, 2] or natural apatites [3, 4]. By natural apatite; e.g. those calcium phosphates which are present in some phosphate rocks, in teeth and bone tissues of animals [5]. Uptake of heavy metals by hydroxyapatite (Hap) involves ion-exchange with calcium ions and also a dissolution–precipitation process [6, 7]. Nevertheless the formation of very small fine particles is often occurs which lead to reduce the interstitial volume in either a column process or at least will require an ultrafiltration one [8]. In batch mode, these fine particles form a suspension and their sedimentation takes much time (several hours) [1]. To perform the separation of suspended particles, one should either conduct an ultrafiltration process or a simple chemical add or a natural substance, in order to accelerate the sedimentation [9, 10]. However, using chemicals to treat water pollution may generate additional waste, therefore, will solve a problem by creating another [11, 12]. Taking in account this problematic, it should be on the use of natural substances such as natural wastes in water pollution treatment.

In this study, chitosan (produced from shrimp waste) was used to flocculate turbid suspensions resulting from the treatment of water contaminated with heavy metals by adsorption on HA.

Materials and Methods

Hydroxyapatite

Hydroxyapatite was synthesized by the well-known Hayek and Newesely's conventional method [13]. However, $CaCO_3$ was used as a source of calcium instead of $Ca(NO_3)_2$ to avoid the formation of harmful nitrogenoxides during the calcination [12]. A 20 g of $CaCO_3$ were suspended in distilled water (50 mL) and drop in an aqueous solution of $NH_4H_2PO_4$ (50 mL). After 72 h of vigorous stirring at room temperature, the obtained product was filtered, washed with distilled water and oven-dried at 60 °C, with the resultant formation of fine white powder which was calcined at 900 °C in order to convert the unreacted $CaCO_3$ into CaO. This latter was easily removed from the fine white powder and should be washed away at *neutral pH*.

Then, the calcium hydroxyapatites (HA) powder was sieved to produce relatively narrow size distribution in the range of 63 μm; both fractions of the first selection were maintained at HA_0 less than 63 μm and HA_A more than 63 μm. Other HA_p fractions of different particle size were obtained from HA_0 by suspension-sedimentation: 10 g of HA_0 were suspended in 1 L of distilled water and stirred for 5 min. Then, it took *an hour* to *settle*, the supernatant particles were separated then air dried which result in HA_B fraction. Similarly, fractions of decreasing particle size denoted HA_C, HA_D and HA_E were obtained from HA_B, HA_C and HA_D, respectively.

Chitosan

Crustacean's chitin is closely associated with the limestone of the shell, and is covalently bonded to proteins, lipids, carotenoid and pigments. Demineralization was carried out by dipping shrimp shells in 2N (HCl) and stirring for 2 days to remove the produced CO_2, whereas deproteinization was made by alkaline treatment at 80–85 °C using 1N (NaOH). The obtained product was then subjected to bleaching with a slight oxidation using a mixture of H_2O_2/HCl (10 % v/v) [14] for more than 1 h. After these three basic steps, the obtained chitin was washed several times with distilled water and then oven-dried at 50 °C for 24 h. Chitosan was obtained by the deacetylation of chitin which was made by alkaline hydrolysis: an amount of chitin produced by the aforementioned steps is suspended in 45 % NaOH at room temperature for 1 week. The obtained chitosan was then filtered, washed with distilled water until pH stability and oven-dried at 50 °C for 24 h.

Determination of particle size was performed using a Mastersizer 100 (Malvern Instruments) by using the laser diffraction technique to measure the size of particles. It was determined by measuring the intensity of light scattered as a laser beam passes through a dispersed particulate sample. This data is then analyzed to calculate the size of the particles that created the scattering pattern. The determination of specific surface by permeability measurements according to the protocol mentioned by Keyes [15] was performed using a Mastersizer 3000 (Malvern Instruments).

The pH of point of zero charge (pH_{pzc}) for HA_0 was determined by the batch mode [16]. For its characterization the chitosan was analyzed by Infrared Spectroscopy ATI Mattson Genessis II Series FTIR allowing also the evaluation of the degree of acetylation from the ratio A_{1320}/A_{1420} [17]. A molecular weight was also calculated by the Mark–Houwink's equation [18, 19] after determining the intrinsic viscosity by capillary viscometer.

Adsorption of Metal Ions

The adsorption of Cu^{2+} and Zn^{2+} was studied using batch mode under different operative conditions. Metallic solutions were carried out using $Cu(NO_3)\cdot 3H_2O$ and $ZnSO_4\cdot 7H_2O$ product purchased from Merck® 45 mg of hydroxyapatite were added to 15 mL (so 3 g/L) of a metallic solution (either Cu^{2+} or Zn^{2+}) of known

concentration and stirred for an accurate time. The suspension was then filtered through a 0.45 μm filter and *metal ion's concentration in the filtrate was determined* by AAS using a Perkin Elmer 200 spectrometer. The *equilibrium time* was determined by adsorption kinetics for a contact time ranged from 5 to 150 min. The pH was adjusted at the beginning of each experiment with 0.1 M NaOH and/or 0.1 M HCl using a HANNA Instrument (pH 211) pH-meter. The effect of pH on metal adsorption was studied between 3 and 8.

Initial metal concentrations ranged from 20 to 150 mg/L were used to study the effect of metallic charge and the established concentrations of adsorbent were varied between 1 and 5 g/L.

The adsorption efficiency was evaluated by determining the adsorption capacity, q (Eq. 1) or the elimination rate E (Eq. 2).

$$q = \left(\frac{C_0 - C_e}{m}\right)V \quad (1)$$

$$E(\%) = \left(\frac{C_0 - C_e}{C_0}\right) \times 100 \quad (2)$$

where: C_0: initial concentration of metal ions in the solution (mg/L), C_e: residual concentration of metal ions in the solution at equilibrium (mg/L), m: mass of adsorbent (g), V: volume of metal solution (L).

Coagulation–Flocculation

Natural sedimentation of different HA suspensions were first studied by following the decrease of turbidity with time. HA suspensions were prepared by adding 3 g of each specified particle size of HA (HA_0, HA_A, HA_B, HA_C, HA_D and HA_E) in 1 L of distilled water. *Turbidity* units are *expressed in nephelometric turbidity units* (NTU) and measured by using an LP2000 HANNA Instrument turbidimeter. Coagulation–flocculation experiments were carried out through a conventional Jar Test (Janke and Hunkeler®) having 5 agitators and trains with variable speed, each train is equipped with a 1 L beaker. Two important parameters were studied *in optimizing coagulation–flocculation*: dose of chitosan (range from 0.08 to 10 mg/L) and pH (between 4 and 8). Chitosan was used in its soluble form by dissolving 1 g in 100 mL of 1 % (v/v) acetic acid. Each coagulation–flocculation test was carried out as follows: 0.750 g of HA particles were suspended in 250 mL water and the pH was adjusted to the desired value. As soon as a fixed amount of the chitosan solution was added to the suspension, the mixture was strongly stirred at 200 rpm for 3 min. This step was followed by a slow mixing at 45 rpm for 20 min. Thereafter, the solution took to settle for 10–120 min. 10 mL of the supernatant were taken at different settling times and measured for turbidity level.

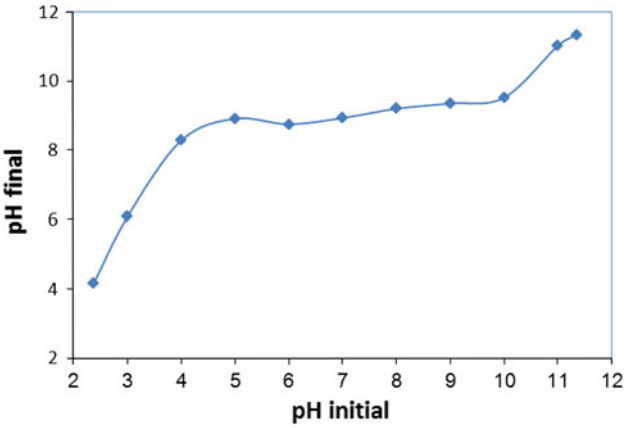

Fig. 1 Determination of pH_{PZC} for hydroxyapatite (HA_0). Inert solution of 0.1 M KNO_3, 3 g/L of adsorbent and 2 h contact time

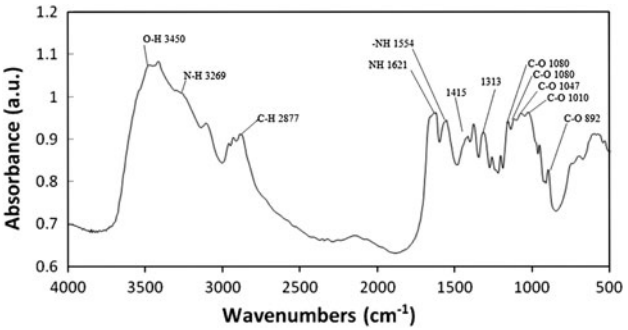

Fig. 2 Infrared spectrum of the prepared chitosan

Table 1 Characteristics of the different hydroxyapatite fractions

Fraction	Density (g/cm^3)	Specific surface area (m^2/g)	Mean diameter (μm)	D_{90} (μm)	D_{50} (μm)
HA_0	–	8	<63	–	–
HA_A	–	/	>63	–	–
HA_B	3	2.4114	52.33	87.77	19.88
HA_C	3	3.4000	2.52	6.90	0.67
HA_D	3	3.8383	1.65	4.47	0.53
HA_E	3	3.6448	5.76	22.50	0.63

Adsorption–Flocculation

In order to assess the efficiency of both adsorption and the coagulation–flocculation by removing heavy metals as well as the turbidity, the coagulation–flocculation process was coupled to the adsorption one reducing the settling time of this process to 30 min (a contact time slightly bigger than the equilibration time previously determined). This contact time achieves at least 90 % elimination rate previously determined and does not match the equilibration time, but it was enough to make technically and economically interesting the process. This was carried out following the adsorption and coagulation–flocculation procedures as described above, i.e. the filtration in the adsorption step was replaced by the coagulation flocculation.

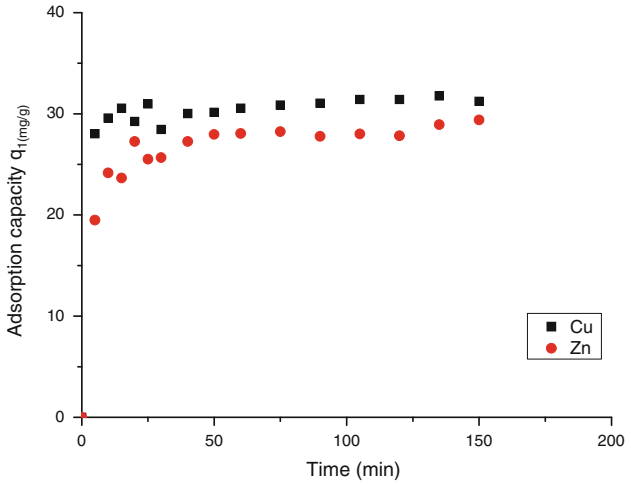

Fig. 3 Effect of contact time on adsorption of Cu^{2+} and Zn^{2+} onto hydroxyapatite. pH 5; $C_0 = 100$ mg/L, $C_A = 3$ g/L

Table 2 Adsorption capacities and their removal extent at equilibrium of Cu and Zn onto hydroxyapatite

Metal ion	Adsorption capacity (mg/g)	Removal extent (%)	Equilibration time (min)
Cu^{2+}	31.4	94.21	105
Zn^{2+}	28.9	87.9	120

Results and Discussion

The results of particle size analysis for HA_0, HA_A, HA_B, HA_C, HA_D and HA_E fractions of hydroxyapatite are reported in Table 1. These results show the possibility of hydroxyapatite powder *fractionation* with smaller particle size less than 63 µm using successive suspension-sedimentation. Average diameters of ca. 52.3, 2.5, 1.6 and 5.7 µm were obtained for HA_B, HA_C, HA_D and HA_E, respectively. The specific surface area is 2.4 m^2/g for HA_B fraction and 3.8 m^2/g for HA_D one, which means higher values of specific surface area correspond to fractions with smaller particle size. It should be noted that the highest value of specific surface area (8 m^2/g) was obtained for HA_0.

However, these values are still lower than those reported by various authors, for example 0.1–85 m^2/g [4], 34–76 m^2/g [6] and 24 m^2/g [7]. Nevertheless, all these values were obtained by the BET method using nitrogen adsorption and can not be compared to the one obtained by laser granulometry, it surely underestimates the area measured by BET method.

Besides it should be noted that the values reported by several authors are for the raw apatite, and in our case; for

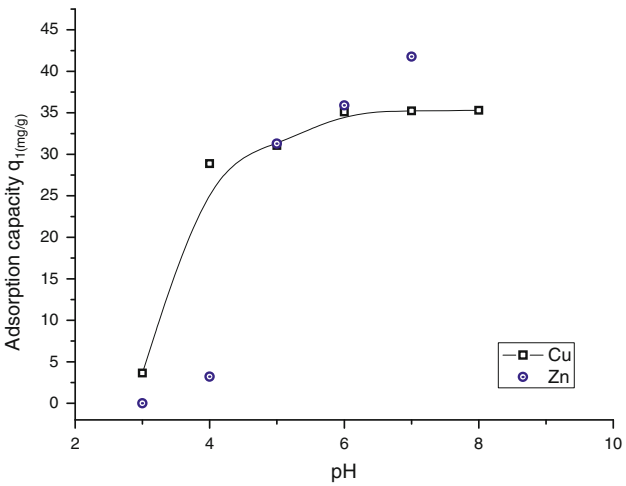

Fig. 4 Effect of initial pH of the solution on adsorption of Cu and Zn on hydroxyapatite. t = 120 min, $C_A = 3$ g/L C_0: 100 mg/L

Table 3 Correlation coefficients of the two kinetic models

	Kinetics of the pseudo-first order			Kinetics of the pseudo-second order			
	R^2	k_1	q_{ecal}	R^2	k_2	q_{ecal}	h
Cu^{2+}	0.8837	0.0244	/	0.9996	0.0162	31.85	16.39
Co^{2+}	0.7508	0.0537	/	0.9975	0.1089	31.95	111.11
Zn^{2+}	0.8432	0.0350	/	0.9923	0.0099	29.50	8.61

both calcined and uncalcined product; surface area depends widely on the duration and the temperature of the calcination [12].

The density of all the HA fractions, equal to 3 g/cm^3, was found to be independent on the particle size and close to the reference value 3.219 g/cm^3 [19].

The results of the determination of the point of zero charge (pH_{pzc}) of hydroxyapatite (HA_0) are shown in Fig. 1. For pH range from 1 to 4.5 and from 10 to 12; the final pH values increased with increasing of initial pH values, whereas the final pH remained fairly constant by varying initial pH from 4.5 to 10. Therefore, hydroxyapatite has good pH and buffering capacity ranging from pH 4.5 to 10. As shown in Fig. 1, this invariability of final pH forms a steady plateau around pH 9.2 ± 0.2 which corresponds to pH of point of zero charge (pH_{pzc}). Such as basic pH_{pzc} was also obtained by Dimovic et al. [4] and its high value is justified by the use of high temperature during the calcination, which generates calcium oxides.

The absorption spectrum of the obtained chitosan is given in Fig. 2. It exhibits the same characteristics peaks that we found in the literature [17, 21, 22].

It can be also established that chitosan is in high purity. Indeed, it's confirmed by the absence of the protein impurities peak at 1,540 cm^{-1} [4, 22]. The degree of deacetylation (DOD) of chitosan is 79.96 %. This value indicates a good quality of deacetylation and therefore highlights the polycationic nature of chitosan. The molecular weight (MW) of prepared chitosan is equal 435.5 kDa. The advantage resulting from this high MW would be a good flocculation as chitosans which involved in these treatments have MW between 100 and 500 kDa [21].

Adsorption of Cu^{2+} and Zn^{2+} onto Hydroxyapatite

Adsorption Kinetics

Figure 3 shows the effect of contact time on adsorption of Cu^{2+} and Zn^{2+} onto hydroxyapatite; the adsorption of Cu^{2+} ions on hydroxyapatite was relatively fast: over 90 % of Cu^{2+} ions were removed from the solution after only 20 min of contact time. However, the elimination of 85 % of Zn^{2+} ions were occurred after 50 min. Adsorption capacities for both metals ions were determined at equilibrium and the results are given in Table 2.

During the experiments of adsorption kinetics, changing the pH of the solution was recorded (results not shown). In fact, adsorption of Cu and Zn onto HA is commonly led to a steady increase in pH until a stable equilibrium value that remains lower than pHpzc. This behavior, on the one hand, can be suitably explained in terms of the buffering capacity of hydroxyapatite which helps to raise the pH of the solution close to its basic pHpzc values, on the other hand, the mechanism of metal ions adsorption onto hydroxyapatite involves an ion-exchange process between metal ions in solution and both Ca^{2+} and H^+ in HA lattice. The released H^+ ions tend to decrease barely the pH of the solution but the buffering capacity of hydroxyapatite outweighs the effect of H^+, consequently, the overall increase in pH during the adsorption.

The values of adsorption rate constants, k_1 and k_2, initial rates, h, and the calculated adsorption capacities at equilibrium, q_{ecal}, are given in Table 3 for both models. As shown in Table 3 and Fig. 3, pseudo-second order is the most suitable kinetic model for the adsorption of Cu^{2+} and

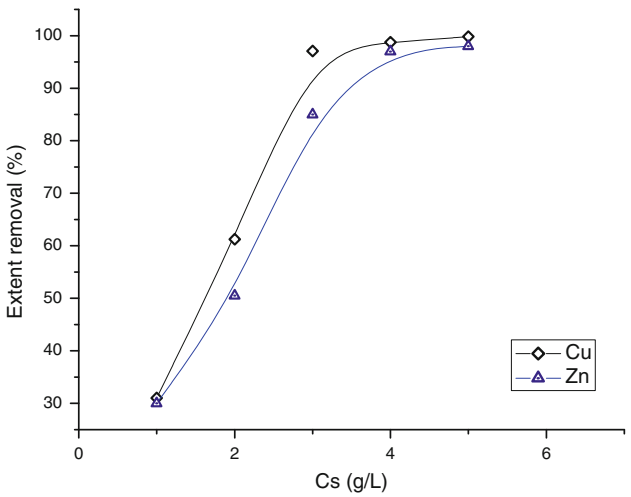

Fig. 5 Effect of initial concentration of adsorbent on the adsorption of Cu and $Zn_{t_{eq}}$ = 120 min, pH = 5, C_0 (metal) = 100 mg/L

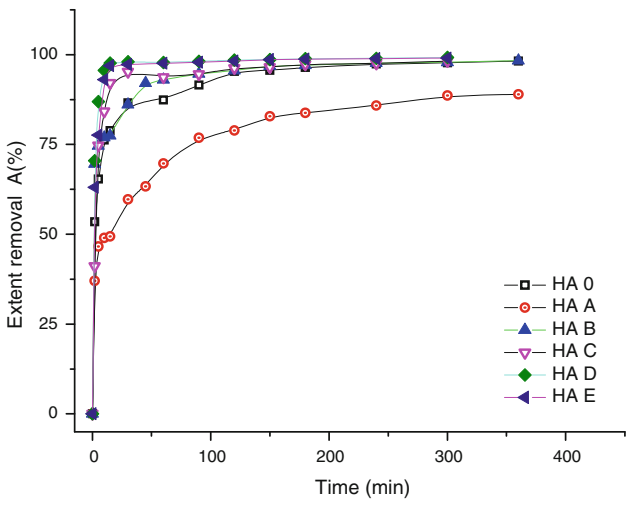

Fig. 6 Natural sedimentation of turbid hydroxyapatite suspensions of different HA particle sizes (HA_0, HA_A, HA_B, HA_C, HA_D and HA_E), C_A = 3 g/L

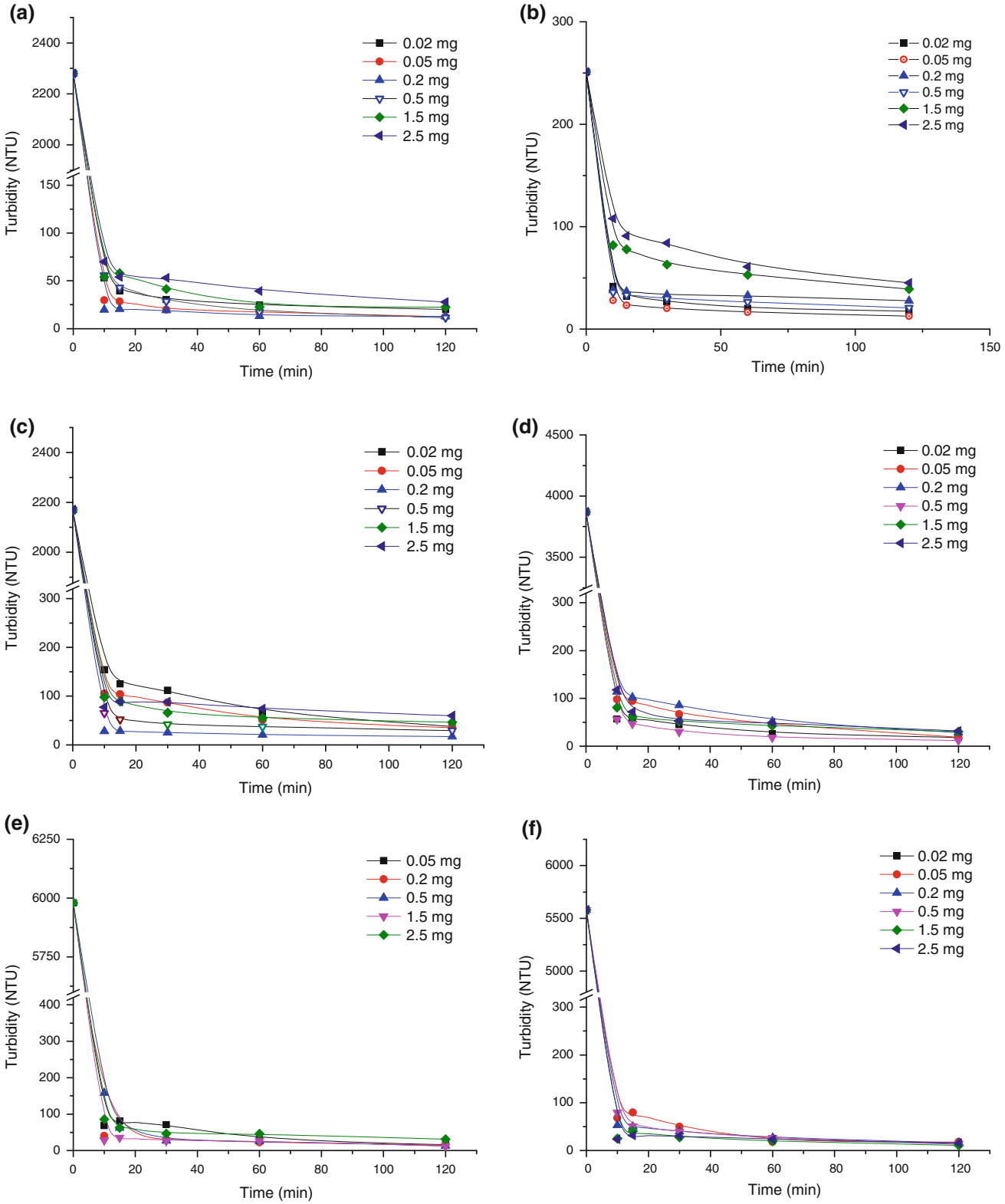

Fig. 7 Effect of chitosan dose on sedimentation kinetics of different hydroxyapatite. **a** HA_0, **b** HA_A, **c** HA_B **d** HA_C, **e** HA_D and **f** HA_E. Conditions: pH 7, $v_1 = 200$ rpm for 3 min, $v_2 = 45$ rpm for 20 min, V = 250 mL

Table 4 Residual turbidity and reduction rate of HA fractions for optimal conditions of coagulation-flocculation (30 min of settling)

HA fraction	Optimal dose of chitosan (mg/250 mL)	Optimal pH	Residual turbidity (NTU)	Extent of removal (%)
HA_A	0.05	7	27.07	91.90
HA_0	0.05	6	19.57	99.14
HA_B	0.2	7	29.24	98.65
HA_C	0.5	7	35.29	99.09
HA_D	0.5	8	47.97	99.19
HA_E	0.5	7	57	98.98

Zn^{2+} on hydroxyapatite. It also allowed us to deduce the theoretical value of the adsorption capacity in each case (Table 3). It should be noted that these calculated values are very close to experimental values. Therefore this model was in good agreement with the experimental results.

To determine the rate constants of adsorption kinetics, data were analyzed using two well known kinetic models, namely the model of pseudo-first order proposed by Lagergren [23] and the pseudo-second order of Ho and McKay [24]. The agreement of a model with experimental results is derived from the values of correlation coefficient R^2.

The values of adsorption rate constants, k_1 and k_2, initial rates, h, and the calculated adsorption capacities at equilibrium, q_{ecal}, are given in Table 3 for both models.

As can be seen from Table 3, the correlation coefficient R^2 for the pseudo-first-order kinetic model at the various temperatures was found to be situated between. 0.7508 and 0.8837. Also, the equilibrium uptake (qe) values calculated from the pseudo-first-order kinetic model did not agree well with the experimental ($qe_{,exp}$) values (values not shown). It was also noticed that the correlation coefficient, R^2, for the pseudo-second-order rate equation was greater (0.99–1), It is in the range of 0.9923–0.9996 and the theoretical q_{ecal} values were closer to the experimental $q_{e,exp}$ values. Based on these results, it can be concluded that the pseudo-second-order kinetic model provided a good correlation for the sorption for the adsorption of Cu^{2+} and Zn^{2+} on hydroxyapatite. This conclusion is in agreement with literature [25–27].

Effect of pH on Metal Sorption

Adsorption of metal ions on hydroxyapatite is strongly influenced by the pH which involves on different types of mechanisms such as: ion-exchange, complexation and retention by electrostatic forces. Adsorption of Cu and Zn on hydroxyapatite at different pH values is illustrated in Fig. 4. The results show that the adsorption capacity increased with pH. This behavior was observed for both metals. Thus, at pH 3 the adsorption capacity was almost nil for both Cu and Zn. It reached high values of about 31 mg/g at pH varied from 5 to 6 and remains constant at pH 7 and pH 8. Indeed, at very acidic pH, metal cations tend to be exchanged with Ca^{2+} and H^+ of the apatitic network, so they are in competition with H^+ ions present at high concentration in the solution. Due to their small size and their mobility as well, H^+ ions are much better sorbed on surface sites of the adsorbent. At alkaline pH, cations metal-removal rate, close to 100 % has been shown. This is due to the precipitation of metal hydroxides [4]. However, for slightly acid to neutral pH (5–7), removed metal would be higher due to ion-exchange that occurs between metal ions and Ca^{2+} of the hydroxyapatite. An optimum adsorption at the range pH of 5–6 was determined from previous results.

Effect of Hydroxyapatite Concentration

As shown in Fig. 5, the metal removal rates by hydroxyapatite increased with the amount of adsorbent. Thus, almost all metal ions (ca. 100 %) were removed by 1 g of HA suspended in 250 cm^3 (C_s = 4 g/L) of metal solution. Unlike removal rate, the adsorption capacity of hydroxyapatite decreased gradually by increasing the amount of adsorbent in contact with metals. This can be related to the saturation of the adsorbent at low solid/liquid ratio.

Flocculation of Turbid Hydroxyapatite Suspensions

In order to evaluate the flocculating effect of chitosan, the natural sedimentation kinetics of hydroxyapatite suspensions were performed. Reduction rate (A) was calculated according to Eq. 3.

$$A\ (\%) = \left(\frac{T_0 - T}{T_0}\right) \times 100 \quad (3)$$

where; T_0 and T are initial and final turbidity, respectively.

Figure 6 shows the turbidity evolution of hydroxyapatite suspensions with time during natural sedimentation. In all cases, suspended particles seem to *settle quickly* during the first 5 min. However, *after 6 h* of sedimentation, a total reduction of turbidity of 98 % was reached. At the end of sedimentation the final turbidity ranged from 27 to 39 NTU.

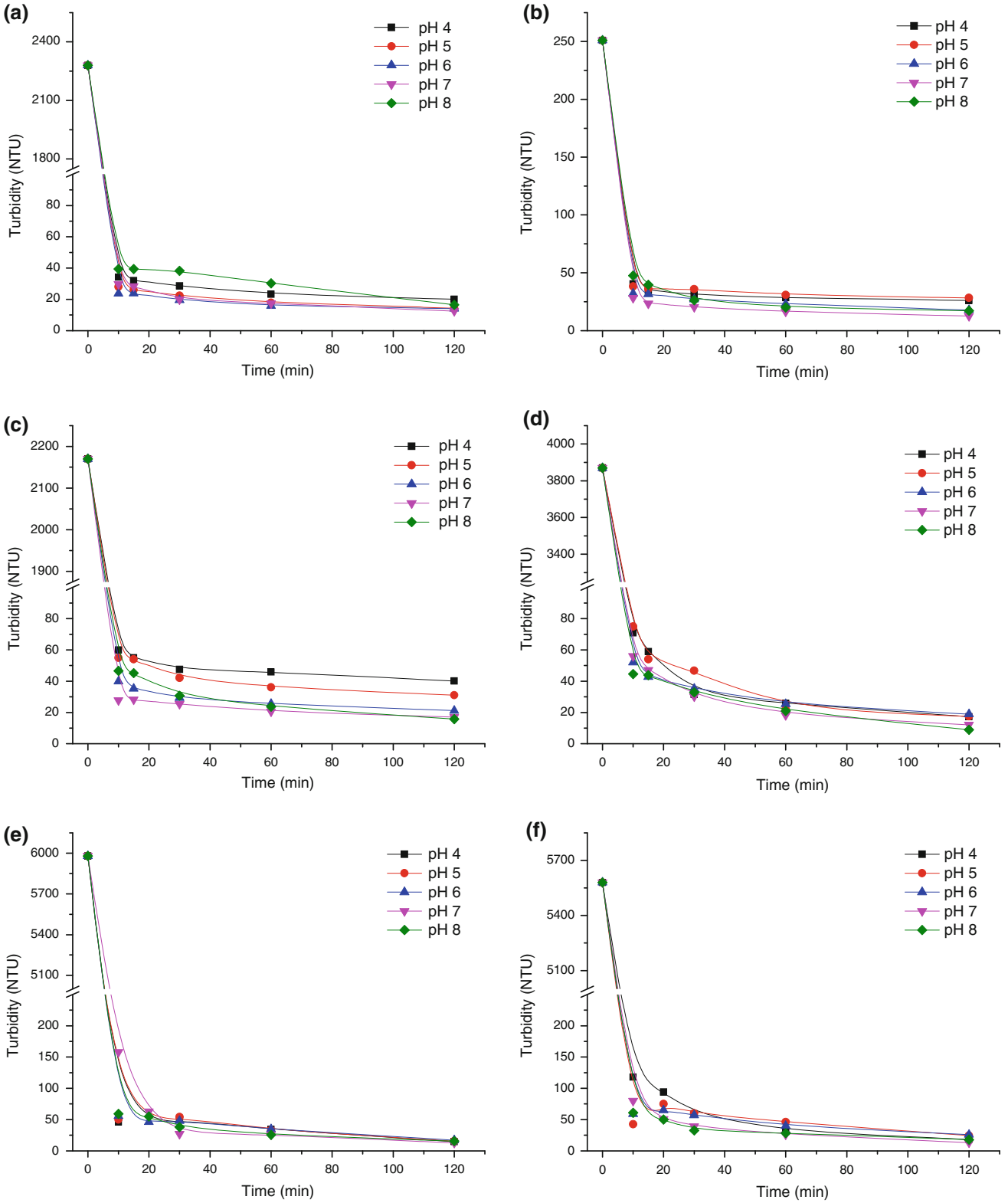

Fig. 8 Effect of pH on sedimentation kinetics of different HA suspensions. Conditions: $v_1 = 200$ rpm for 3 min, $v_2 = 45$ rpm for 20 min, V = 250 mL. **a** HA_0, **b** HA_A, **c** HA_B, **d** HA_C, **e** HA_D and **f** HA_E. Chitosan dose was equal to 0.05 mg for HA_0 and HA_A, 0.2 mg for HA_B and 0.5 for HA_C, HA_D and HA_E

Effect of Chitosan Dose

The results of sedimentation kinetics showed the ability of chitosan to remove turbidity from all suspensions. According to chitosan dose and after 2 h of sedimentation turbidity, which is varied between 11.4 and 60 NTU, corresponds a reduction rate of 99.5 and 97.2 %, respectively.

In order to evaluate the optimum dosage of chitosan, experiments of coagulation–flocculation of different HA suspensions were carried out at pH 7 with different doses of chitosan (ranging from 0.08 to 10 mg per litter of HA suspension) and the results are shown in Fig. 7. Thus, as for quite small and much higher doses, the efficiency of chitosan seems to be decreased. In fact, for higher doses the surface of HA particles will be positively charged due to chitosan adsorption which conduct to the re-stabilization of the suspension.

A large decrease in turbidity was observed during the first 10 min of sedimentation for all samples. The reduction rate was 57 and 99.16 % for HA_A and HA_0, respectively. A very significant removal of turbidity was observed with chitosan doses ranging from 0.05 to 0.5 mg (in 250 mL of HA suspension). The optimal doses of chitosan should be 0.05 mg for HA_0 and HA_A, 0.2 mg for HA_B, 0.5 mg for HA_C, HA_D and HA_E (Table 4). These optimal doses were used for studying the effect of pH.

Effect of pH on Coagulation–Flocculation

A slight decrease in chitosan efficiency was observed at pH 4, 5 and 8 for HA_0, HA_A and HA_B (Fig. 8). The optimal pH for better coagulation–flocculation of HA suspensions was determined by measuring residual turbidity after 30 min of decantation (Table 4). Thus, optimal pH was found equal to 6, 8, and 7 for HA_0, HA_D and the remaining HA fractions, respectively. However, to facilitate coupling processes, both adsorption and flocculation–coagulation, should be performed all experiments at one fixed pH value. Thus, pH 6 was held on for further working up mainly because of it reduction rate which is found in pH range between 6 and 8 (Table 4).

Conclusion

Hydroxyapatite HA has shown his efficiency in removing 88–95 % of the initial charge of Cu and Zn ions with a fast relatively kinetics. However, the using of HA powder generates turbid suspension that requires too much of sedimentation time. To increase the sedimentation velocity, the chitosan was added to metals-loaded HA suspension and acted as a flocculent. Optimal adsorption and sedimentation conditions were determined for all important parameters: pH (pH 6–7), amount of adsorbent (3 g/L), equilibration time (120 min), stirring speed (200 rpm for 3 min followed by 45 rpm for 20 min) and dose of flocculent (0.05–0.5 mg/250 mL). Chitosan has shown high efficiency in removing turbidity of various HA suspensions of different particle size (reduction rate exceeded 98 %). Coupling adsorption and coagulation–flocculation processes had also confirmed the effectiveness of chitosan in removing turbidity, even in the presence of metal ions. Indeed, the reductions rate of *over 99 % corresponding with* the residual turbidity ranged from 10 to 40 NTU. Furthermore, adsorption of metal ions onto hydroxyapatite was not affected by the presence of chitosan. These results are really interesting that underline a new ecological method, it could also be used for the heavy metals recovery.

References

1. Kadouche S, Zemmouri H, Benaoumeur K, Drouiche N, Sharrock P, Lounici H (2012) Metal ion binding on hydroxyapatite (Hap) and study of the velocity of sedimentation. Procedia Eng 33:377–384
2. Corami A, Mignardi S, Ferrini V (2007) Copper and zinc decontamination from single- and binary-metal solutions using hydroxyapatite. J Hazard Mater 146:164–170
3. Kaludjerovic-Radoicic T, Raicevic S (2010) Aqueous Pb sorption by synthetic and natural apatite: kinetics, equilibrium and thermodynamic studies. Chem Eng J 160:503–510
4. Dimovic S, Smiciklas I, Plecas I, Antonovic D, Mitric M (2009) Comparative study of differently treated animal bones for Co^{2+} removal. J Hazard Mater 164:279–287
5. Bolay N, Santran V, Dechambre G, Combes C, Drouet C, Lamure A, Christian R (2009) Production by co-grinding in a media mill, of porous biodegradable polylactic acid–apatite composite materials for bone tissue engineering. Powder Technol 190:89–94
6. Sheha R (2007) Sorption behavior of Zn(II) ions on synthesized hydroxyapatites. J Colloids Interface Sci 310:18–26
7. Šljivić M, Smičiklas I, Plećaš I, Mitrić M (2009) The influence of equilibration conditions and hydroxyapatite physico-chemical properties onto retention of Cu^{2+} ions. Chem Eng J 148:80–88
8. Bellier N, Chazarenc F, Comeau Y (2006) Phosphorus removal from wastewater by mineral apatite. Water Res 40:2965–2971
9. Wang Q, Heiskanen K (1992) Selective hydrophobic flocculation in apatite-hematite system by sodium oleate. Miner Eng 5: 493–501
10. Ozkan A, Uslu Z, Duzyol S, Ucbeyiay H (2007) Correlation of shear flocculation of some salt-type minerals with their wettability parameter. Chem Eng Process 46:1341–1348
11. Andres Y, Faur-Brasquet C, Gérente C, LeCloirec P (2007) Elimination des ions métalliques et des métalloïdes dans l'eau. Techniques de l'ingénieur M 8000:1–14
12. Hadioui M, Sharrock P, Mecherri M, Brumas V, Fiallo M (2008) Reaction of lead ions with hydroxylapatite granules. Chem Papers 62:516–521
13. Hayek E, Newesely H (1963) Pentacalciummonohydroxyorthophosphate-hydroxyapatite. Inorg Synth 7:63–65
14. Kuo-Shien H, Wei J, Dans CC (2007) Effect of pretreatment with low molecular weight chitosanon the dyeability of cotton Fabrics. Res J Textile Apparel 11:54–59

15. Keyes WF (1946) Determination of specific surface by permeability measurements. Ind Eng Chem Anal Ed 18(1):33–34
16. Smičiklas I, Onjia A, Raičević S, Janaćković Đ, Mitrić M (2008) Factors influencing the removal of divalent cations by hydroxyapatite. J Hazard Mater 152:876–884
17. Kasaai MR (2008) A review of several reported procedures to determine the degree of N-acetylation for chitin and chitosan using infrared spectroscopy. Carbohydr Polym 71:497–508
18. Kasaai MR (2007) Calculation of Mark–Houwink–Sakurada (MHS) equation viscometric constants for chitosan in any solvent–temperature system using experimental reported viscometric constants data. Carbohydr Polym 68:477–488
19. Motta de Moura C, Motta de Moura J, Soares NM, Almeida Pinto LA (2011) Evaluation of molar weight and deacetylation degree of chitosan during chitin deacetylation reaction: used to produce biofilm. Chem Eng Process 50:351–355
20. Rey C, Combes C, Drouet H, Sfihi A, Barroug C (2007) Physicochemical properties of nanocrystalline apatites: implications for biominerals and biomaterials. Mater Sci Eng, C 27:198–205
21. Zemmouri H, Kadouche S, Lounici H, Hadioui M, Mameri N (2011) Use of chitosan in coagulation flocculation of raw water of Keddara and Beni Amrane dams. Water Sci Technol Water Supply 11:202–210
22. Crini G, Gimbert F, Capucine C, Martel B, Adam O, Morin-Crini N, De Giorgi F, Badot PM (2008) The removal of Basic Blue 3 from aqueous solutions by chitosan-based adsorbent: batch studies. J Hazard Mater 153:96–106
23. Schüürmann G (1991) First-order and pseudo-first-order elimination kinetics. Sci Total Environ 109:110395–110405
24. Ho YS, McKay G (1999) Pseudo-second order model for sorption processes. Process Biochem 34:451–465
25. Sairam Sundaram C, Viswanathan N, Meenakshi S (2008) Defluoridation chemistry of synthetic hydroxyapatite at nano scale: equilibrium and kinetic studies. J Hazard Mater 55: 206–215
26. Elkady MF, Mahmoud MM, Abd-El-Rahman HM (2011) Kinetic approach for cadmium sorption using microwave synthesized nano-hydroxyapatite. J Non-Cryst Solids 357:1118–1129
27. Xu HY, Yang L, Wang P, Liu Y, Peng MS (2008) Kinetic research on the sorption of aqueous lead by synthetic carbonate hydroxyapatite. J Environ Manage 86:319–328